ZIBELINE INTERNATIONAL™ PUBLISHING

ISSN: 2521-0858 (Print)
ISSN: 2521-0866 (Online)
CODEN: SHJCAS

Science Heritage Journal (GWS)

DOI: http://doi.org/10.26480/gws.02.2024.73.78

RESEARCH ARTICLE

EQUATORIAL TOTAL ELECTRON CONTENT'S (TEC) REACTION TO GEOMAGNETIC STORM EVENTS FROM JANUARY TO MARCH 2020.

Adebayo, Samuel[a], Ajide, Adeolu Bamidele[b], Babatola, Babatunde Keji[c]

[a]Physics Department, University of Ilorin, Ilorin, Nigeria
[b]Physics Department, University of Uyo, Uyo, Nigeria.
[c]Physics Unit, Science Laboratory Department, Osun State Polytechnic, Iree, Nigeria.
Corresponding Author Email: adephy2000@hotmail.com

ARTICLE DETAILS

Article History:

Received 13 February 2024
Revised 17 March 2024
Accepted 21 April 2024
Available online 30 July 2024

ABSTRACT

This study looked at the behaviour of Equatorial Total Electron Content (TEC) in connection to geomagnetic storms that occurred between January and March of 2020. The data used in the study came from the Global Positioning System (GPS). Vertical Total Electron Content (VTEC) data was collected at three different ground stations to conduct the investigation: NKLG (GMAGLat. -8.04°S, GMAGLong. 81.05°E), ADIS (GMAGLat. 1.13°N, GMAGLong. 110.47°E), and DJIG (GMAGLat. 3.36°N, GMAGLong. 11457°E). The locations were carefully chosen in order to offer a comprehensive picture of the equatorial ionosphere's response to magnetic storms. The study's findings show that the equatorial region undergoes both amplification and depletion effects in the reaction of TEC to geomagnetic storms. The paper also proposed possible approaches to clarify these findings. The three stations' different latitudinal positions were recognised as the principal source of the considerable variations in GPS-TEC responses during storm periods. Furthermore, during the storm periods, the peak positive percentage deviation of TEC displayed an ascending trend with rising altitude for each monitoring station. This finding suggests the existence of complex height-related interactions between the equatorial ionosphere and geomagnetic storms. The current study examines the complicated factors that influence the behaviour of TEC in equatorial regions during geomagnetic storms. It highlights the need of adding latitudinal and altitude factors in such studies.

KEYWORDS

Magnetic Storm Response, Dual-Frequency GPS, Latitudinal Differences, Geomagnetic Storm Mechanisms, Altitude-Dependent Variations

1. INTRODUCTION

Our solar system, a huge expanse of celestial bodies held together by the gravitational attraction of the Sun, contains not only the Sun itself but also the planets, asteroids, and comets that orbit it (Lichtenberg et al., 2021). Among these cosmic friends, the Earth maintains a particular place as the sole known sanctuary for life. Situated at an average distance of around 150 million kilometers (93 million miles) from the Sun, Earth travels along an elliptical orbit, causing the distance between our planet and its radiant star to change significantly over the year (Waltham, 2019).

Although the Sun may be considered an average star in terms of size and luminosity, its proximity to Earth provides it an apparent magnitude and brilliance unequaled by most other stars in our cosmic neighborhood. To put this into perspective, if we were to assemble Earth's diameter of around 1.4 million kilometers (or 860,000 miles) by linking individual Earths in a linear fashion, it would require a staggering 110 Earths lined up end to end (Willmer, 2018). One key feature of our Earth's atmospheric dynamics is in its ionosphere an area in the upper atmosphere ionized by solar radiation. This ionization process occurs when photons released by the Sun clash with atoms and molecules in the ionosphere, freeing electrons and positively charged ions. The resulting electron density has a tremendous impact on the transmission of radio waves, a phenomenon defined as Total Electron Content (TEC) (Habarulema et al., 2021).

The equatorial TEC, particularly, counts the total number of electrons across a unit cross-sectional area running from the Earth's surface to the ionosphere along the planet's magnetic field lines. However, the TEC is not static; it is vulnerable to the influence of geomagnetic storms, which result from solar activity. These storms hurl high-energy particles into Earth's magnetosphere, creating disturbances in the ionosphere and modifying the TEC (Shinbori et al., 2020). During geomagnetic storms, the ionosphere receives heightened ionization, particularly around the equatorial area. This phenomenon, known as the equatorial ionization anomaly, manifests as peaks of ionization on either side of the magnetic equator. As geomagnetic storms worsen, the equatorial ionization anomaly strengthens, resulting in increasing rates of ion formation (Idolor et al., 2021).

The repercussions of these ionospheric perturbations transcend beyond scientific interest. The Global Positioning System (GPS), upon which modern navigation and communication systems significantly rely, depends on radio signals traversing the ionosphere. Consequently, changes in equatorial TEC during geomagnetic storms can affect GPS operation, resulting to signal delays, positioning mistakes, and related problems (Dabbakuti et al., 2019).

By studying oscillations in equatorial TEC during geomagnetic storms, scientists get vital insights into ionospheric dynamics and disruptions. Such observations not only enrich our understanding of Earth's atmospheric dynamics but also contribute to the development of robust ionosphere-dependent technologies required for modern communication and navigation systems (Akala et al., 2020).

1.1 Total Electron Content (TEC)

Currently, a wide range of techniques are employed to investigate the

Quick Response Code	Access this article online	
	Website: www.jscienceheritage.com	**DOI:** 10.26480/gws.02.2024.73.78

Cite the Article: Adebayo, Samuel, Ajide, Adeolu Bamidele, Babatola, Babatunde Keji (2024). Equatorial Total Electron Content's (TEC) Reaction to Geomagnetic Storm Events from January to March 2020. *Science Heritage Journal, 8(2): 73-78.*

characteristics of the equatorial ionosphere. Academic institutions and similar establishments often possess the necessary resources and equipment to undertake novel investigations pertaining to ionospheric characteristics, such as electron density and TEC(Shehu et al., 2018). Additionally, these technologies can be employed for the ongoing monitoring of scintillations. The aggregate electron content (AEC), particularly in the spatial region connecting the satellite and the receiver, is the summation of all unbound electrons included within a unit area measuring 1 m^2. The ability to grasp the complexity of the ionosphere necessitates a vital descriptive quality. The concept of multiple TEC units refers to a scenario in which there are many units of thermal electric coolers (TECs) present ($TECU = 10^{16}, m^{-2}$) (Huang et al., 2019).

TEC is obtained using GPS receivers. The TEC is described by:

$$TEC = \int_0^R N_e \, ds \quad (1)$$

Where N_e= electron density, s = path length of the signal propagated, TEC is an important ionospheric parameter and can be greatly influenced by solar weather. TEC measurements are produced by GPS.

1.2 Geomagnetic Storm

A geomagnetic storm is a large-scale disturbance of the Earth's magnetosphere that is caused by solar activity. The Earth is constantly bombarded by solar wind, which consists of a magnetic field and a continual stream of particles emitted by the solar system. This material is frequently shielded by the Earth's self-generated magnetic field (Pezzopane et al., 2019). High-speed, high-density solar wind episodes can produce intermittent perturbations in the Earth's magnetic field. These disturbances have the power to create currents in the upper atmosphere, which results in atom excitation and the creation of auroras in the northern and southern regions. This occurrence causes a geomagnetic storm. Geomagnetic storms affect the thermosphere, causing changes in the neutral composition of this atmospheric layer (Cai et al., 2020).

METHODOLOGY

The GPS-TEC data used in this investigation were obtained by downloading them in Receiver Independent Exchange (RINEX) format from the repository of the African Geodetic Reference Frame (AFREF) Station Web Server, accessible at http://www.afrefdata.org. Subsequently, the RINEX data were subjected to analysis utilising the GPS-TEC retrieval technique (version 2.9.3 of the GPS_GOPI software), developed by Gopi Krishna Seemala from the Institute of Scientific Research at Boston College in Boston, USA (Okoh et al., 2019).

The RINEX files that were obtained were then accessed using the GOPI programme. The essential TEC dataset is subsequently acquired by using each of these files. The extracted data is stored in an own folder. This folder contains a file with the extension (*.CMN), a file with the extension (*. Bias), a file with the extension (*.std), and six (6) PNG pictures (Baca et al., 2018). The TEC files that have been approximated may be found within the CMN file. The RINEX files are calculated using the bias values of the satellite and receiver, which are stored in the Bias file. The daily average TEC files are stored within the STD file (Rino et al., 2019). The aforementioned documents are

The TEC data from three equatorial stations in both hemispheres of the African sector have been studied to investigate the TEC response during this time of storm activity. The GPS readings from the IGS database were obtained and afterwards evaluated (Oyedokun et al., 2021). The reception locations are positioned in the northern hemisphere, specifically in Libreville (NKLG), Addis Abeba (ADIS), and Djibouti (DJIG) (Simwanda et al., 2019). The NKLG station is located to the south of the geomagnetic equator, as seen in Figure 1.

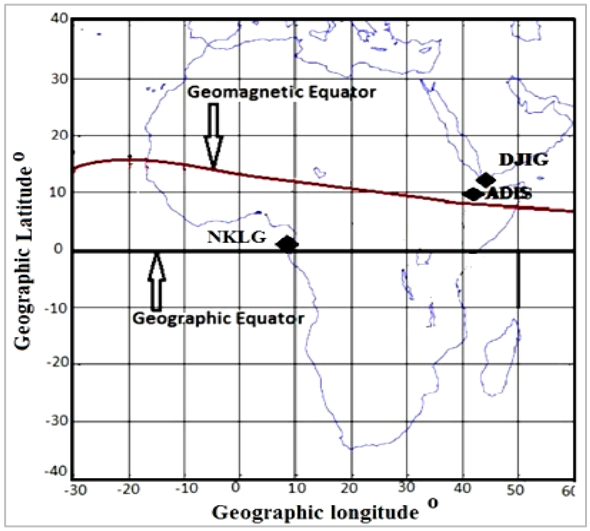

Figure 1: Map of Africa showing locations of the IGS receiver stations that were used in this research work.

The VTEC was derived from the downloaded RINEX data using the GPS-TEC retrieval technique developed by Gopi Krishna Seemala from the Institute of Scientific Research at Boston College in Boston, USA. The data was retrieved, organised onto a notepad, and afterwards transferred to an Excel spreadsheet (Mehmood et al., 2019).

The study found the 10 days with the least magnetic activity during the storm period. The average TEC levels for these days were then plotted against Universal Time (UT). The storm study additionally used the hourly VTEC data values from the three (3) locations. All storm days within the designated months were accompanied by GPS data (Shinbori et al., 2020). These figures were derived from the AFREF Reference Station Web archive (http://www.afrefdata.org), which is accessible to the general public online. The mean TEC values were computed and plotted against UT. Subsequently, the diurnal variation plots of VTEC were generated for the specified period of eight days, encompassing the days of storm activity occurring around two days prior (Tariku, 2020).

The calculation of the percentage departure of storm time %Δin TEC from the reference value (quiet-time value) is determined by the equation (2) provided (Kundu et al., 2020):

$$\%\Delta \text{ in TEC} = \frac{\text{TEC}_{\text{observed}} - \text{TEC}_{\text{ref}}}{\text{TEC}_{\text{ref}}} \times 100 \quad (2)$$

where $\text{TEC}_{\text{observed}}$ is the observed hourly value of TEC and TEC_{ref} is the reference value for each hour.

The reference values for periods of calm are determined by taking the average hourly measurements from the ten (10) least magnetically active days of the month during which the storm occurred (Alabdulgader et al., 2018). In order to see the occurrence of an ionospheric storm, it is necessary for both positive and negative effects to manifest continuously for a minimum duration of three hours, with the magnitude of the percentage deviation above 20%. The study project utilised the following tools: MATLAB, GPS_GOPI_v_2.9.3 software, and Microsoft Office Excel (Wang et al., 2021).

3. RESULT AND DISCUSSION

The analysis of the TEC graphs for all stations throughout the period of January to March reveals some unexpected characteristics. Based on the data shown in Figure 2, it can be noticed that the plots from January 2020 had a notable decrease in enhancement compared to the plots from February and March 2020 (Kundu et al., 2020).

During the period of analysis including January to March 2020, the NKLG station consistently exhibited elevated levels of Total Electron Content Units (TECU) during the nocturnal hours, namely from midnight until just

before daybreak. In the period of nighttime hours, the recorded values exhibited a low of about 9.22 TECU in March 2020, a high of about 11.34 TECU in February 2020, and a value of around 10.07 TECU in January. A decline in these values was recorded, followed by an augmentation at around 4:00 UT throughout the period spanning from January to March 2020.

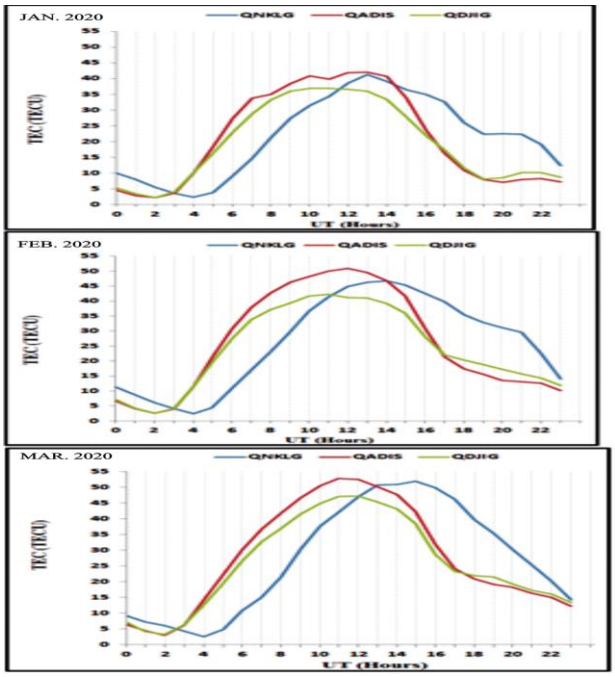

Figure 2: Quiet day plots for all stations during January – March 2020

Based on the information provided in Figure 2, it can be observed that the quiet TEC plots for the ADIS and DJIG stations had overlapping characteristics throughout the overnight hours from January to March 2020. The aforementioned pattern in both stations remained consistent until the early hours before to sunrise, where a noticeable divergence began to manifest at 5:00 UT throughout the months of January and February. The discrepancy began to manifest only in the month of March, commencing at around 4:00 UT. The maximum values across all stations were observed. The aforementioned figures were observed during the hours of 11:00 and 15:00 UT. According to Figure 3, the NKLG station had a maximum value of around 41.28 TECU in January 2020. In February 2020, a post-noon peak value of around 46.79 TECU was recorded. In March 2020, a post-noon peak value of approximately 51.93 TECU was observed. The ADIS station documented the highest recorded levels.

3.1 Response of TEC to Storm

The shape of the VTEC recorded during geomagnetic storm occurrences exhibits variations compared to the plots found during periods of low geomagnetic activity (Kundu et al., 2020). Furthermore, the diurnal variation of VTEC may be categorised into three separate stages: the build-up stage (0500 to 0900UT), the daylight stage (0900 to 1800UT), and the nocturnal stage (1800 to 0500UT). The plots derived from the days characterised by disturbances were juxtaposed with those originating from the days marked by tranquilly, yielding the subsequent findings. Upon considering all the plots, it becomes evident that there is no observable alteration in TEC during the build-up phase. Nevertheless, fluctuations were seen specifically during the daytime hours (0900-1800 UT) in close proximity to sunset, as well as on days characterised by stormy weather.

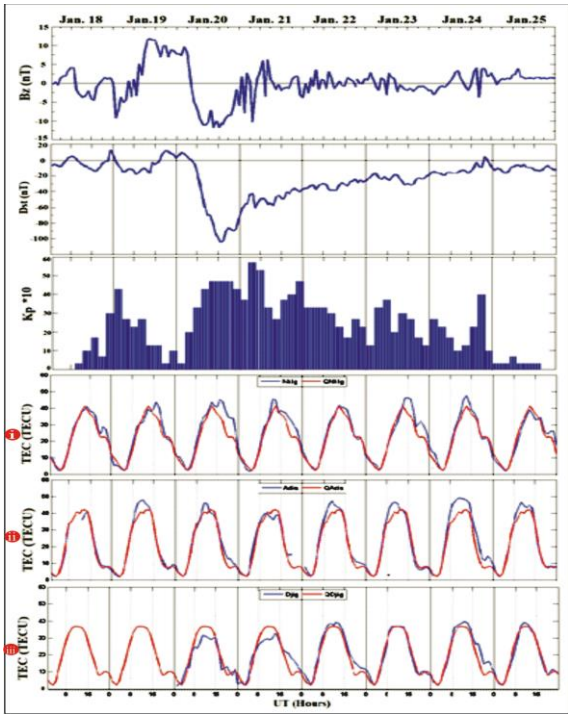

Figure 3: During the storm event in January 2016, there were variations in the IMF's southbound component (Bz), Dst index, three-hourly Kp index, and the averaged diurnal monthly variation of TEC for the (i) NKLG (ii) ADIS (iii) DJIG stations. January 18–25, 2020, is when the action takes place.

From Figure 3. The response of NKLG Station to a January storm was significant, with double peaks observed during the daytime on the storm day (20 Jan. 2020). ADIS Station experienced a significant increase in TECU during the daytime interval (0900-1800UT). DJIG Station experienced a depression in TECU with two peaks occurring between about 0900-1600 UT on the storm day (20 Jan. 2020). During the night, no increase in TECU was observed on the storm day (20 Jan. 2020)

From figure 4. The response of NKLG, ADIS, and DJIG stations to a February storm is shown in Fig. 4(a). NKLG station experienced a significant enhancement in the TECU during the daytime period, while ADIS observed a single peak during the day time of the stormy day (16 Feb. 2020). DJIG observed enhancements in TECU throughout the storm period, with double peaks occurring frequently between 0900-1600 UT. On the storm day (16 Feb. 2020), the TECU was slightly increased during the main phase. During the night, a sharp increase in TECU was observed at about 1900UT on 16 Feb. 2020 which later dropped on the same day.

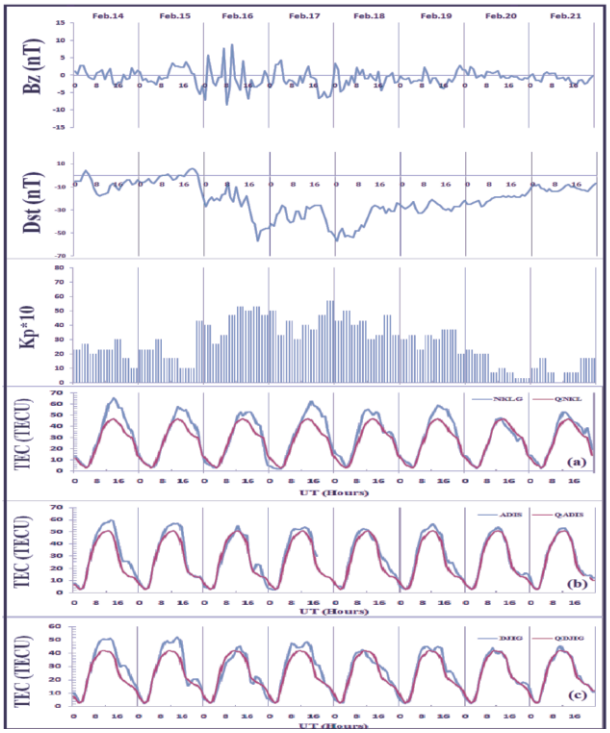

Figure 4: shows how the IMF's southbound component (Bz), Dst index, three-hourly Kp index, and averaged diurnal monthly variation of TEC for the (a) NKLG (b) ADIS (c) DJIG stations changed during the storm event in February 2020. 14 to 21 February 2020 are covered by the story.

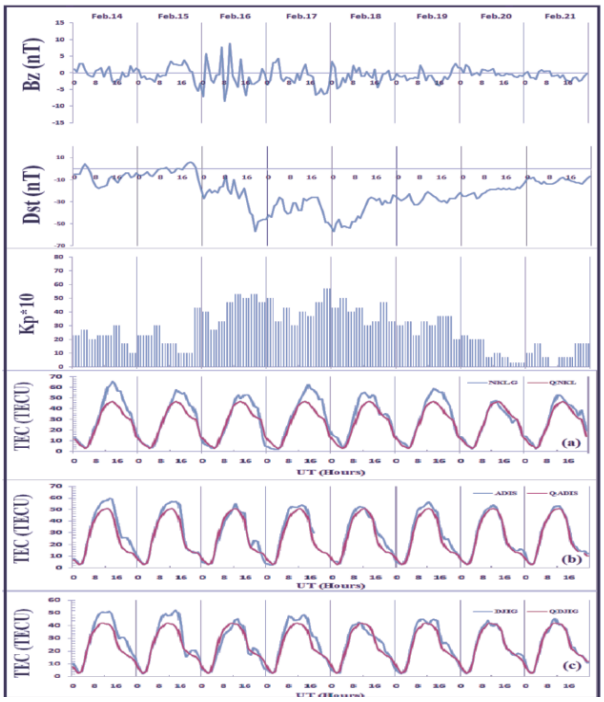

Figure 5: Variability of the IMF's southbound component (Bz), the three-hourly Kp index, the Dst index, and the averaged diurnal monthly variation of TEC for the (a) NKLG (b) ADIS (c) DJIG stations during the storm event of March 15–17, 2020. The story takes place between March 4 and March 11, 2020.

From Figure 5. The response of NKLG, ADIS, and DJIG stations to March storms was observed in Fig. 5 (a). NKLG station experienced a significant enhancement in TECU during the daytime interval (0900-1800UT). ADIS station experienced a significant depression in TECU during the daytime interval (0900-1600UT). DJIG station experienced a slight increase in TECU during the daytime interval (0900-1800UT). During the night, a sharp increase in TECU was observed with peak at about 2000UT.

4. Conclusion

This study's primary objective was to investigate the differences in GPS-TEC across a subset of African stations. This investigation focused on three specific geomagnetic occurrences. Three equatorial/low-latitude stations were chosen for the investigation: Addis Abeba (ADIS), Djibouti (DJIG), and Libreville (NKLG). NKLG is specifically located south of the

geomagnetic equator. The results of the study disclosed a complex response of the thermosphere-ionosphere system to geomagnetic disturbances, characterised by both increases and decreases in the TEC in this region. During the entire investigated geomagnetic storm, it was observed that the NKLG station exhibited a more pronounced TEC reaction than the ADIS and DJIG stations. During periods of cyclone activity, the percentage deviation of TEC data showed a similar upward trend with increasing altitude across all stations.

The examination of TEC graphs from January to March revealed an interesting pattern. The dynamic nature of the ionospheric response to geomagnetic conditions was highlighted by the fact that the TEC enhancement decreased in January, followed by a notable increase in February and March.

The examination of TEC values during specified time intervals yielded additional insights. Throughout the duration of the investigation, the NKLG station consistently exhibited elevated TEC values during the nighttime (from midnight to dawn). The observed values for the months of January, February, and March fluctuated within the range of 10.07 TECU to 11.34 TECU. During the time period between January and March, TEC values decreased, followed by an increase around 4:00 UT. The TEC patterns observed at the ADIS and DJIG stations were comparable during nighttime hours, but distinct differences were observed around 5:00 UT in January and February, and 4:00 UT in March. The highest total electron content (TEC) values were recorded between 11:00 and 15:00 UT during diurnal periods. NKLG reported the highest values, with maximums of approximately 41.28 TECU in January, 46.79 TECU in February, and 51.93 TECU in March.

Upon examining the effect of geomagnetic storms on TEC, it was discovered that the VTEC profiles varied between storm occurrences and periods of minimal geomagnetic activity. The study uncovered three distinct stages: the build-up stage, which occurred between 0500 and 0900 UT; the daylight stage, which occurred between 0900 and 1800 UT; and the twilight stage, which occurred between 1800 and 0500 UT. During the initial phase, there were no significant changes in TEC, but fluctuations were observed during daylight hours close to sunset and on days with severe weather.

Throughout January, February, and March, the observed responses of NKLG, ADIS, and DJIG stations to geomagnetic storms exhibited discernible patterns. During daytime hours, NKLG displayed a significant increase in TEC enhancement, whereas ADIS displayed a single apex. During the storm phases, DJIG exhibited significant increases and decreases in TEC, manifested as two distinct maxima. In this way, the complex ionospheric response to geomagnetic disturbances has been clarified.

REFERENCE

Akala, A. O., Oyeyemi, E. O., Amaechi, P. O., Radicella, S. M., Nava, B., and Amory-Mazaudier, C. 2020. Longitudinal Responses of the Equatorial/Low-Latitude Ionosphere Over the Oceanic Regions to Geomagnetic Storms of May and September 2017. Journal of Geophysical Research: Space Physics, 125 (8). https://doi.org/10.1029/2020ja027963

Alabdulgader, A., McCraty, R., Atkinson, M., Dobyns, Y., Vainoras, A., Ragulskis, M., and Stolc, V., 2018. Long-Term Study of Heart Rate Variability Responses to Changes in the Solar and Geomagnetic Environment. Scientific Reports, 8 (1). https://doi.org/10.1038/s41598-018-20932-x

Baca, T., Turecek, D., McEntaffer, R., and Filgas, R., 2018. Rospix: modular software tool for automated data acquisitions of Timepix detectors on Robot Operating System. Journal of Instrumentation, 13(11), Pp. C11008–C11008. https://doi.org/10.1088/1748-0221/13/11/c11008

Cai, X., Burns, A. G., Wang, W., Qian, L., Solomon, S. C., Eastes, R. W., Pedatella, N., Daniell, R. E., and McClintock, W. E. (2020). The Two-Dimensional Evolution of Thermospheric ∑O/N2 Response to Weak Geomagnetic Activity During Solar-Minimum Observed by GOLD. Geophysical Research Letters, 47(18). https://doi.org/10.1029/2020gl088838

Dabbakuti, J. K., Mallika, Y., Venugopala Rao, M., Raghava Rao, K., and Venkata Ratnam, D., 2019. Modeling of GPS-TEC using QR-decomposition over the low latitude sector during disturbed geomagnetic conditions. Advances in Space Research, 64(10), Pp. 2088–2103. https://doi.org/10.1016/j.asr.2019.08.020

Habarulema, J. B., Okoh, D., Bergeot, N., Burešová, D., Matamba, T., Tshisaphungo, M., Katamzi-Joseph, Z., Pinat, E., Chevalier, J. M., and Seemala, G., 2021. Interhemispheric comparison of the ionosphere and plasmasphere total electron content using GPS, radio occultation and ionosonde observations. Advances in Space Research, 68 (6), Pp. 2339–2353. https://doi.org/10.1016/j.asr.2021.05.004

Huang, C. Y., Helmboldt, J. F., Park, J., Pedersen, T. R., and Willemann, R., 2019. Ionospheric Detection of Explosive Events. Reviews of Geophysics, 57(1), Pp. 78–105. https://doi.org/10.1029/2017rg000594

Idolor, O. R., Akala, A. O., and Bolaji, O. S., 2021. Responses of the African and American Equatorial Ionization Anomaly (EIA) to 2014 Arctic SSW Events. Space Weather, 19(11). https://doi.org/10.1029/2021sw002812

Kundu, S., Sasmal, S., Chakraborti, S., and Chakrabarti, S. K., 2020. Study the Ionospheric Total Electron Content (TEC) variation during Geomagnetic Storm in 24th Solar Cycle. *2020 URSI* Regional Conference on Radio Science (URSI-RCRS). https://doi.org/10.23919/ursircrs49211.2020.9113605

Lichtenberg, T., Drążkowska, J., Schönbächler, M., Golabek, G. J., and Hands, T. O., 2021. Bifurcation of planetary building blocks during Solar System formation. Science, 371 (6527), Pp. 365–370. https://doi.org/10.1126/science.abb3091

Mehmood, M., Naqvi, N. A., and Saleem, S., 2019. GPS Total Electron Content (TEC) estimation using single station measurements. *2019* Sixth International Conference on Aerospace Science and Engineering (ICASE). https://doi.org/10.1109/icase48783.2019.9059214

Okoh, D., Seemala, G., Rabiu, B., Habarulema, J. B., Jin, S., Shiokawa, K., Otsuka, Y., Aggarwal, M., Uwamahoro, J., Mungufeni, P., Segun, B., Obafaye, A., Ellahony, N., Okonkwo, C., Tshisaphungo, M., and Shetti, D., 2019. A Neural Network-Based Ionospheric Model Over Africa from Constellation Observing System for Meteorology, Ionosphere, and Climate and Ground Global Positioning System Observations. Journal of Geophysical Research: Space Physics, 124 (12), Pp. 10512–10532. https://doi.org/10.1029/2019ja027065

Oyedokun, O., Akala, A., and Oyeyemi, E., 2021. Responses of the African equatorial ionization anomaly (EIA) to some selected intense geomagnetic storms during the maximum phase of solar cycle 24. Advances in Space Research, 67(4), Pp. 1222–1243. https://doi.org/10.1016/j.asr.2020.11.020

Pezzopane, M., Del Corpo, A., Piersanti, M., Cesaroni, C., Pignalberi, A., Di Matteo, S., Spogli, L., Vellante, M., and Heilig, B., 2019. On some features characterizing the plasmasphere–magnetosphere–ionosphere system during the geomagnetic storm of 27 May 2017. Earth, Planets and Space, 71(1). https://doi.org/10.1186/s40623-019-1056-0

Rino, C., Morton, Y., Breitsch, B., and Carrano, C., 2019. Stochastic TEC Structure Characterization. Journal of Geophysical Research: Space Physics, 124(12), Pp. 10571–10579. https://doi.org/10.1029/2019ja026958

Shehu, M., Said, R., and Okoro, E., 2018. The trend of ionospheric total electron content near the equator. Bayero Journal of Pure and Applied Sciences, 10(1), Pp. 258. https://doi.org/10.4314/bajopas.v10i1.52s

Shinbori, A., Otsuka, Y., Sori, T., Tsugawa, T., and Nishioka, M. (2020). Temporal and Spatial Variations of Total Electron Content Enhancements During a Geomagnetic Storm on 27 and 28 September 2017. *Journal of Geophysical Research: Space Physics*, *125*(7). https://doi.org/10.1029/2019ja026873

Simwanda, M., Ranagalage, M., Estoque, R. C., & Murayama, Y. (2019). Spatial Analysis of Surface Urban Heat Islands in Four Rapidly Growing African Cities. Remote Sensing, 11(14), Pp. 1645. https://doi.org/10.3390/rs11141645

Tariku, Y. A., 2020. Pattern of the variation of the TEC extracted from the GPS, IRI 2016, IRI-Plas 2017 and NeQuick 2 over polar region, Antarctica. Life Sciences in Space Research, 25, Pp. 18–27. https://doi.org/10.1016/j.lssr.2020.02.004

Tariq, M. A., Shah, M., Hernández-Pajares, M., and Iqbal, T., 2019. Ionospheric VTEC variations over Pakistan in the descending phase of solar activity during 2016–17. Astrophysics and Space Science, 364(6). https://doi.org/10.1007/s10509-019-3591-3

Waltham, D., 2019. Is Earth special? Earth-Science Reviews, 192, Pp. 445–470. https://doi.org/10.1016/j.earscirev.2019.02.008

Wang, H., He, Y. F., Lühr, H., and Zhang, J., 2021. Local Time and Longitudinal Differences in the Occurrence Frequency of Ionospheric EMIC Waves During Magnetic Storm Periods. Journal of Geophysical Research: Space Physics, 126 (2). https://doi.org/10.1029/2020ja028878

Willmer, C. N. A., 2018. The Absolute Magnitude of the Sun in Several Filters. The Astrophysical Journal Supplement Series, 236(2), Pp. 47. https://doi.org/10.3847/1538-4365/aabfdf